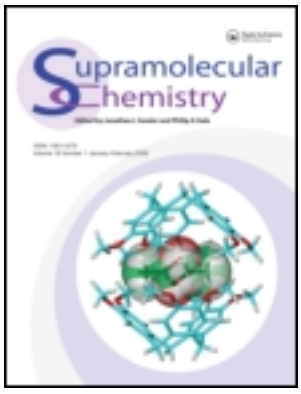

Supramolecular Chemistry
Publication details, including instructions for authors and subscription information:
http://www.tandfonline.com/loi/gsch20

Interplay of solvent in flexible behaviour of cyclohexane dinapthyl *bis*-thiourea system: conformational aspects

Avijit Pramanik [a] & Gopal Das [a]
[a] Department of Chemistry, Indian Institute of Technology, Guwahati, Assam, 781 039, India

Available online: 03 May 2011

To cite this article: Avijit Pramanik & Gopal Das (2011): Interplay of solvent in flexible behaviour of cyclohexane dinapthyl *bis*-thiourea system: conformational aspects, Supramolecular Chemistry, 23:6, 425-434

To link to this article: http://dx.doi.org/10.1080/10610278.2010.544734

Supramolecular Chemistry
Vol. 23, No. 6, June 2011, 425–434

Interplay of solvent in flexible behaviour of cyclohexane dinapthyl *bis*-thiourea system: conformational aspects

Avijit Pramanik and Gopal Das*

Department of Chemistry, Indian Institute of Technology, Guwahati, Assam 781 039, India

(*Received 12 May 2010; final version received 26 November 2010*)

Trans-1,2-*bis*-3-(naphthalen-1-yl) thioureido cyclohexane (**L**) compound is a new host material with considerable structural adaptability over a range of solvents. An investigation of the binding behaviours of solvents to the flexible host **L** was carried out in the solid phase as well as in the solution phase. The formation of these solvent-induced polymorph and the structural similarities and dissimilarities in their packing motifs can be rationalised through multipoint solute–solvent non-covalent interactions. In addition to strong hydrogen bonds, different types of non-covalent intermolecular C—H···O, C—H···S, N—H···S C—H···π, π···π and lone pair···π interactions were found to stabilise the crystal structures. Powder X-ray diffraction, thermal analysis and optical microscopic studies were performed to support the crystallographic studies. Solvent-dependent NMR spectroscopy shows significant change in the peak position with changes in the solvents. Furthermore, solution-phase photo-physical (especially steady state and time-resolved fluorescence) studies were also carried out to emphasise the role of the solvent polarity on the conformational flexibility of the host through non-covalent interactions.

Keywords: host–guest chemistry; conformational analysis; self-assembly; NMR; fluorescence

Introduction

Solvent-induced polymorphism (*Pseudo*-polymorphism) is a common phenomenon in drug targets and biological molecules (*1*, *2*). Pseudo-polymorphism, a subject of interest in supramolecular chemistry, has various potential applications in separations, sensing, storage and catalysis (*3*). Solvent-induced polymorphism has potential impact on bulk properties and crystal habit (*4*). Because of their different physical and chemical properties, solvents not only influence the crystal growth rate and the final morphology but also have an effect on polymorphism via solute–solvent interactions (*5*, *6*). Nature of solvents and solvent–host interactions can contribute to the stability of the solvated crystals, i.e. the final pseudo-polymorph (*7*). Recently, we have undertaken research investigations on thiourea derivatives because of its outstanding applications in the field of supramolecular chemistry (*8*, *9*). Electro-neutral thiourea receptors contain multiple hydrogen-bonding sites which help non-specific binding of solvent molecules (*10*). The relatively acidic thiourea NH protons (*11*), with a strong hydrogen bond donor capability, can establish multipoint hydrogen-bonding patterns with complementary acceptor groups in a specific and predictable manner. Thiourea containing two *thio*-ureido-NHs has potential hydrogen bond donors for the assembly-solvated host–guest complex. Moreover, the diffusiveness of the electronic charge in the lone pairs of sulphur leads to the thiocarbonyl group being a weak hydrogen-bonding acceptor, unlikely to interfere in conformational or complexing studies involving other stronger acceptor centres (*12*). Furthermore, receptors with flexible multi-podal structure favours formation of stable host–guest complexes due to their favourable geometry and higher dimensional orientation (*13*).

In our continuing effort towards design and synthesis of multi-podal host systems capable of forming neutral complexes with guests of different dimensionality (*14*), we report here the existence of at least three different solvatomorphs of chiral *trans*-1,2-*bis*-3-(naphthalen-1-yl)-thioureido cyclohexane (**L**; Scheme 1). In the present paper, we have shown that two thioureido-NHs have taken a major role for the construction of pseudo-polymorphic a structure of nathyl-based *thio*-urea system. Non-covalent interactions in the solid state will be different when using different solvents with the same ligand. These results yield different crystal morphology. We have also rationalised the solvent-induced conformational adaptability of **L** in solid and solution phases with various polarities of the solvent. Powder X-ray diffraction (PXRD) analysis, NMR experiments and thermal studies were also performed. In addition, solvent-dependent photo-physical properties of **L** were thoroughly investigated for conformational flexibility through various supramolecular interactions through host–guest complexes in the solution phase.

*Corresponding author. Email: gdas@iitg.ernet.in

ISSN 1061-0278 print/ISSN 1029-0478 online

DOI: 10.1080/10610278.2010.544734
http://www.informaworld.com

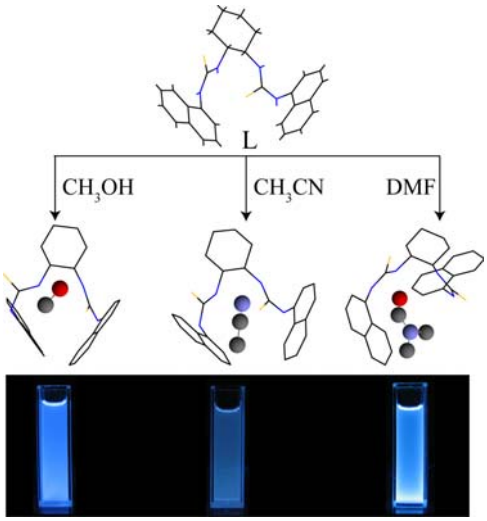

Scheme 1. Schematic representation of conformational adaptability in solvated *trans*-1,2-*bis*-(3-(naphthalen-1-yl) thioureido cyclohexane (**L**).

Results and discussion

Crystal structure studies

Cyclohexyl group retains its most favourable chair conformation in all three reported structures as reported earlier (*15*). Methanol enters into the crystal lattice of **L** via hydrogen bonding (Figure 1(a)) in the channel (7.16 × 7.71 Å) along *a*-axis (Figure 1(b)), which accommodates solvent dimer. Dimeric MeOH molecules stacked in opposite orientation via C—H···O interactions (Figure 1(c)). Each dimer is separated by 7.17 Å along *a*-axis and 10.32 Å along *b*-axis. One of the NH attached to cyclohexyl unit form N—H···O hydrogen bond with MeOH, which also forms O-H···S type hydrogen bond with neighbouring thiourea unit. Complementary N-H—S bond resulted in the formation of 1D hydrogen-bonded chain diagonally along the *bc* plane. Napthyl moieties are oriented in the opposite direction (see Supplementary Information, available online). Neighbouring molecules are linked by thioamide–thioamide hydrogen-bonding interactions forming a 1D chain along *c*-axis (see Supplementary Information, available online), which is common in thiourea compounds and its derivatives (*16*, *17*). Each thiourea unit has a common *syn* and *anti* geometry. Both the *anti* conformations have a similar close to 180°dihedral angle (Table 1). However, one of the *syn* N—H conformations has dihedral angle very close to 0°, whereas the other is little larger (6.87°). The FT-IR spectrum of the crystal shows O—H stretching vibrations of MeOH at around 3300 cm^{-1}.

Similar observations were found in the acetonitrile-solvated system (Figure 2(a)). Flexible host **L** reorganises themselves to accommodate larger and linear MeCN in the crystal lattice. 1D channel along *a*-axis and solvent dimer in each cavity is observed, as in the previous case (Figure 2(b)). The cavity size is larger (9.73 × 7.83 Å) to accommodate the larger MeCN solvent molecule. MeCN forms N—H···N, C—H···N and C—H···π-type non-covalent interactions with the ligand (Figure 2(c)). However, in contrast to the MeOH crystal, non-covalent interactions between the solvent molecules are not observed as such. In the MeOH-solvated crystal, *syn* conformation is more deviated than that of MeCN-solvated crystal (Table 1). The FT-IR spectrum of the crystal shows $\nu_{C\equiv N}$ bands at 2100 and 2356 cm^{-1}.

The switch from MeOH or MeCN to DMF, a solvent of higher dimensionality containing amide group had a dramatic effect on the conformation of the host molecule and the network structure (Figure 3(a)). Larger DMF molecule exists as a monomer (Figure 3(b)) within a cylindrical cavity (9.58 × 7.96 Å). In contrast to the previous crystals, here naphthalene unit forms C—H···S-type bond with thiourea unit (see Supplementary Information, available online). Each DMF molecule is stacked between two naphthalene rings in the solid state and C—O group is pointed towards the thiourea unit (see Supplementary Information, available online). This particular orientation of the DMF molecules helps in the formation of two rare types of non-covalent interactions viz. C—O···π *(18)* and lone pair (lp)···π (*18*, *19*; Figure 3(c)) interactions with the naphthalene unit in addition to the common N—H···O-type hydrogen bonds (see Supplementary Information, available online). The FT-IR spectrum of the crystal shows a lower C—O stretching frequency at 1680 cm^{-1} than an unsubstituted C—O bond. Also, peaks at 1500, 1250, 1120 and 860 cm^{-1} are because of the partial double-bond character, the rotation about the C—N bond. In this case, we have seen significantly more deformation of *syn* and *anti* conformation of the dihedral angle of S—C—N—H bonds than the previous systems (Table 1).

Comparisons of all the pseudo-polymorphic structures are presented in Figure 4. For easy comparison in the 3D conformation of the flexible ligand, all the solvent molecules are omitted and the cyclohexyl unit is shown in the most stable chair conformation. Relative orientation of C—S groups in the pendent arms largely differ in the case of the MeOH-solvated system. However, relative orientation of the naphthalene units is similar in unsolvated ligand and MeCN-solvated crystal. In other two solvated crystals, these two aromatic rings are oriented in a different manner and large deviation is observed in DMF-solvated crystal.

Crystal habit

Different crystallisation parameters such as the solvent polarity (*20*) and the average levels of supersaturation are important to obtain a desired crystal habit, which is an

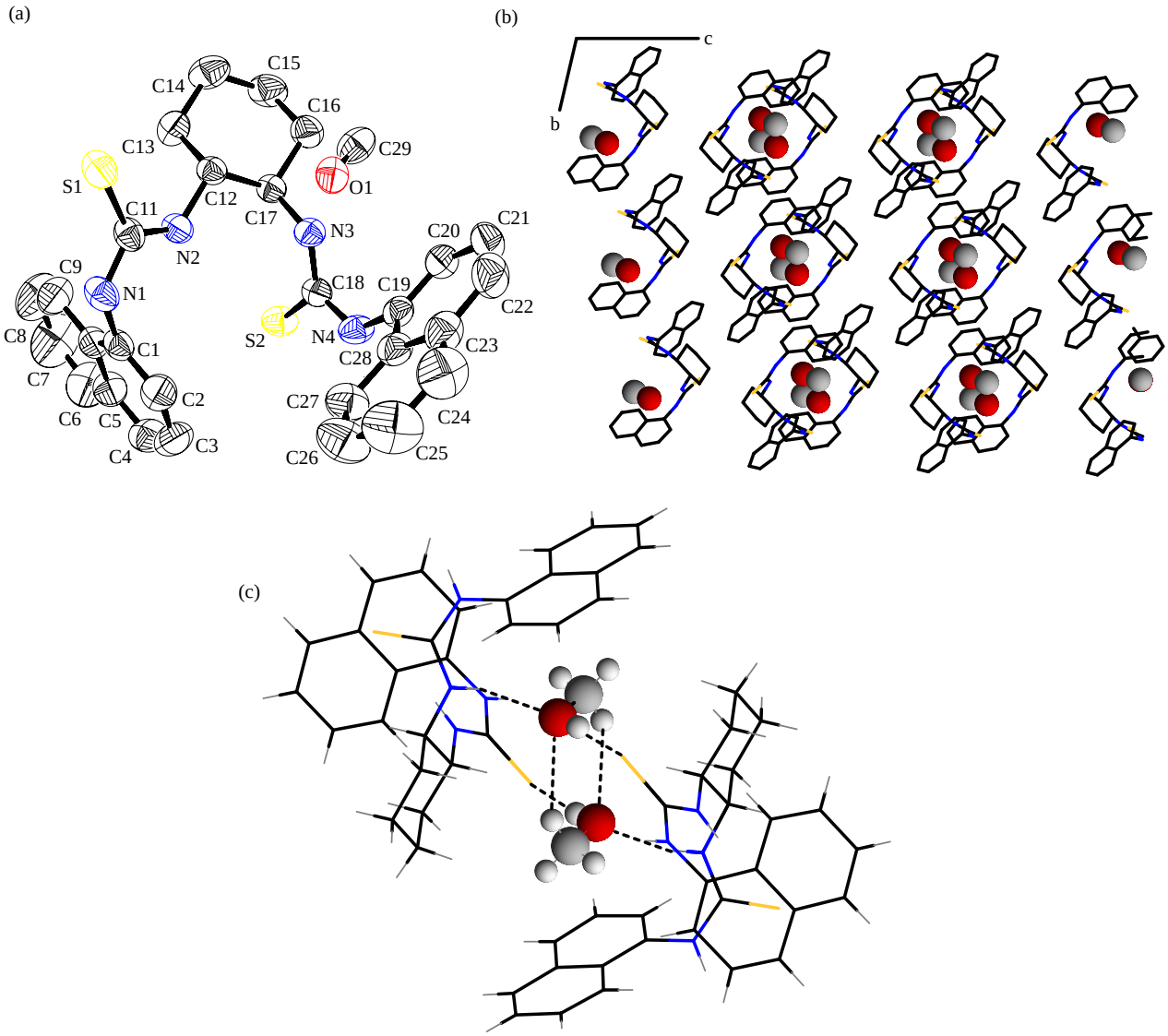

Figure 1. (a) ORTEP view of **L·MeOH** with atom labelling scheme (hydrogen atoms are omitted for clarity); (b) Packing diagram highlighting the guest dimer in the channel and (c) MeOH dimer formation via C—H···O interaction.

important manifestation for the quality of the final products besides the crystal structure. Thiourea groups of **L** form different types of non-covalent interactions with the solvent, which are manifested in the crystal morphology (see Supplementary Information, available online).

Thermal analysis

The DSC thermogram of the crystal without solvent was obviously different from the solvated systems as shown in Figure 5. Ligand **L** shows one endothermic peak at ~192°C with an onset temperature of 178°C due to the melting of **L**. The heat of melting was calculated to be 49.3 kJ mol^{-1}. However, in solvated systems, two endothermic peaks were found. The peak at lower temperature, ~112°C for **L·MeOH**, ~138°C for **L·MeCN** and ~170°C for **L·DMF**, was attributed to the desolvation

Table 1. Selected torsion angles and bond angles in the crystals.

Entry	**L·MeOH** (°)	**L·MeCN** (°)	**L·DMF** (°)
S1—C11—N1—H	6.87	3.54	6.97
S1—C11—N2—H	0.54	2.30	1.99
S2—C18—N3—H	2.34	0.28	4.03
S2—C18—N4—H	3.33	2.67	3.04
N2—C12—C17	108.90	107.91	111.29
N2—C12—C13	111.79	111.56	111.10
N3—C17—C12	111.54	110.88	109.76
N3—C17—C16	111.65	111.32	110.72

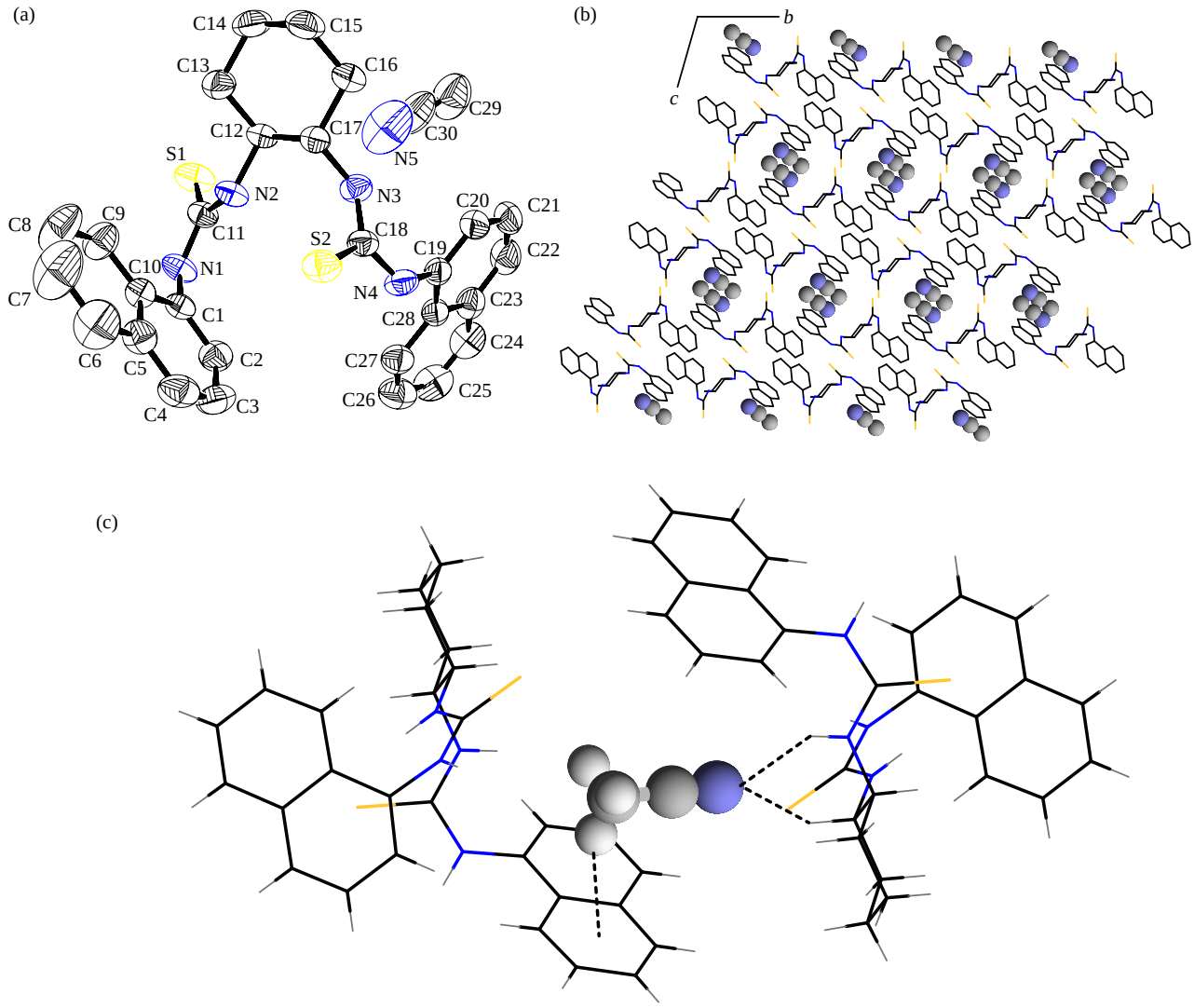

Figure 2. (a) ORTEP view of **L·MeCN** with atom-labelling scheme (hydrogen atoms are omitted for clarity), (b) perspective view highlighting the solvent dimer in the cavities and (c) Non-covalent interaction associated with solvent in the lattice.

process. These peaks are higher than the boiling point of the corresponding solvents, revealing that the solvents had intensive hydrogen-bonding interaction with **L**. These observations are as per the single-crystal X-ray diffraction analysis.

XRD analysis

The PXRD is an important tool to determine the crystalline nature in the bulk sample. PXRD patterns of **L** and solvated crystals were completely different in the position and intensity of the diffraction peaks (Figure S12 of the Supplementary Information, available online). Furthermore, different PXRD patterns also implied that compound crystals might exhibit polymorphs or solvates. These differences in bulk crystalline properties are in agreement with the difference in their crystal structure.

Solvent-dependent NMR spectroscopy

To investigate the supramolecular host–guest interactions in the solution state, we have selected $CDCl_3$, CD_3OD, CD_3CN and DMSO-d_6 solvents (*21*). Figure 6(a) ^{1}H NMR spectra of DMSO-d_6-solvated *bis*-thiourea system which shows sharp Ar–NH peak at ~9.8 ppm, whereas those of the CD_3CN-solvated system shows sharp peak at ~8.2 ppm (Figure 6(b)). Similarly, the sharp peak of the ^{1}H NMR spectra of the $CDCl_3$-solvated system is shown at ~6.3 ppm (Figure 6(d)), whereas a large shift (~4.5 ppm) has been found in CD_3OD (Figure 6(c)). However for aliphatic NH proton, no prominent shift in the peak positions was observed on changing the polarity of the solvents ($\delta = 4.1$ ppm) due to steric constraints. NMR studies support these observations in the solution phase. NMR studies also show the role of two thioureido—NHs for the construction of

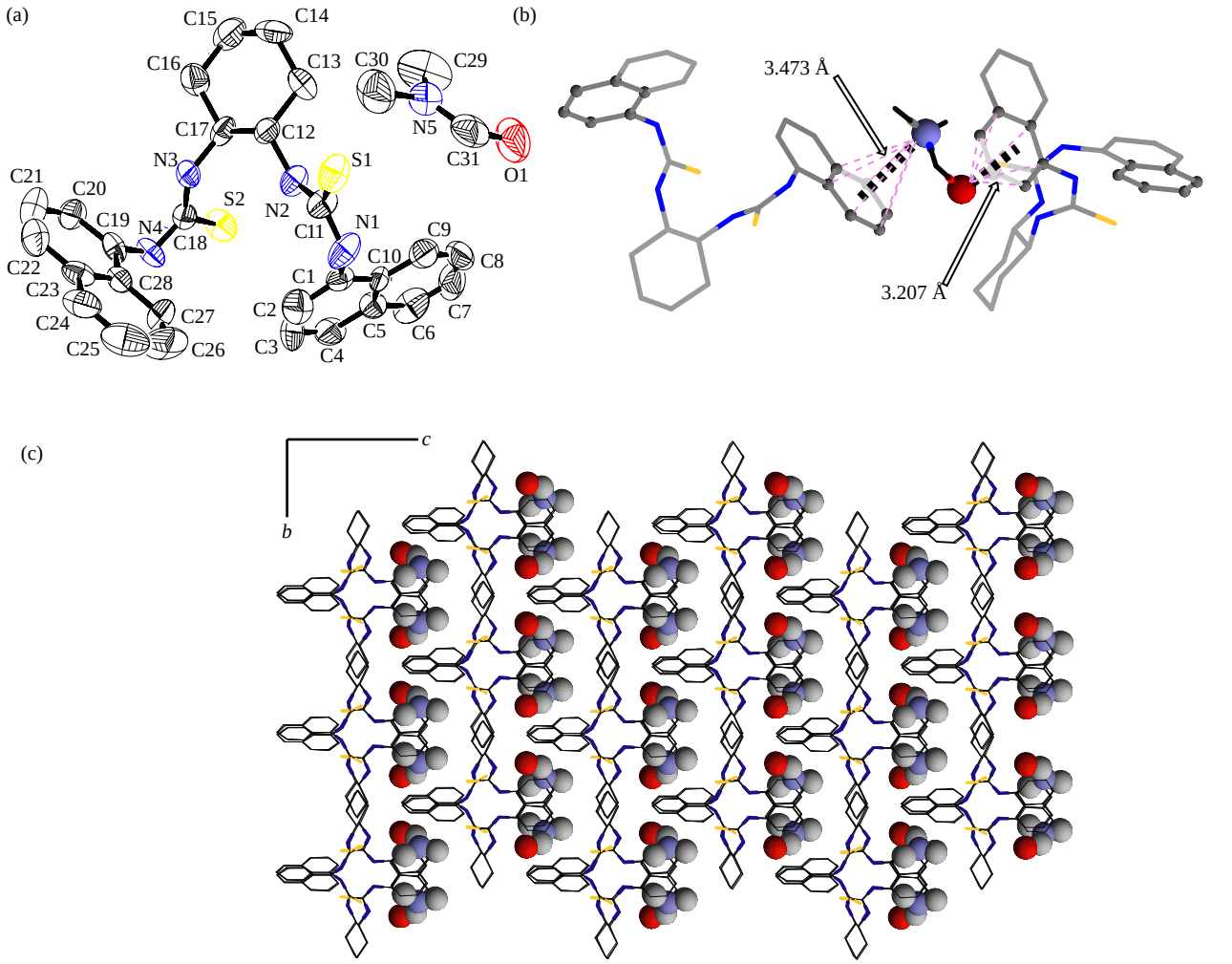

Figure 3. (a) ORTEP view of **L·DMF** with atom-labelling scheme (hydrogen atoms are omitted for clarity), (b) perspective views of the lp $\cdots\pi$ interaction in **L·DMF** via Olp $\cdots\pi$ and Nlp $\cdots\pi$ in DMF molecule and (c) perspective views of **L·DMF** highlighting the guest molecules in the cavities.

pseudo-polymorphic structure of the nathyl-based *thio*-urea system. Weak change in peak positions are observed for other protons in solvated *bis*-thiourea complexes. No significant changes were found in ^{13}C NMR studies. Interestingly, the large change (shift) in peak position ($\delta = \sim 4.5$–9.8 ppm) for aromatic —NH proton is possibly due to the hydrogen-bonding interactions, involving the —NH group attached to the naphthalene ring and solvents of different polarities which is also reflected in the solid-state structures

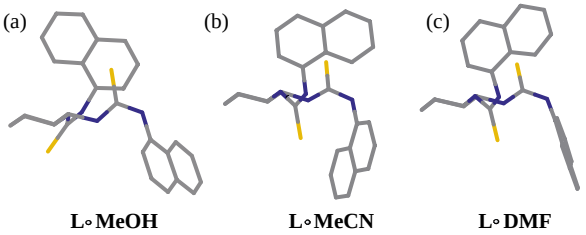

Figure 4. Comparison of different conformations of the ligand in different crystal forms (solvent molecules are removed for clarity).

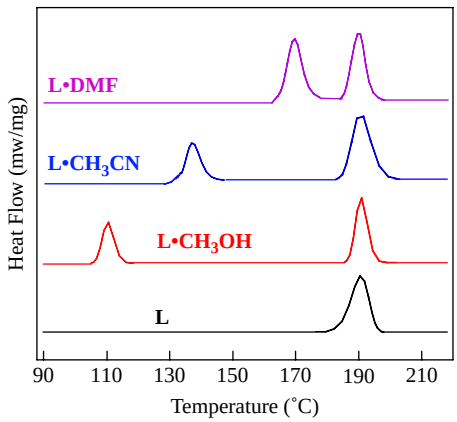

Figure 5. DSC thermograms of different solvated crystals.

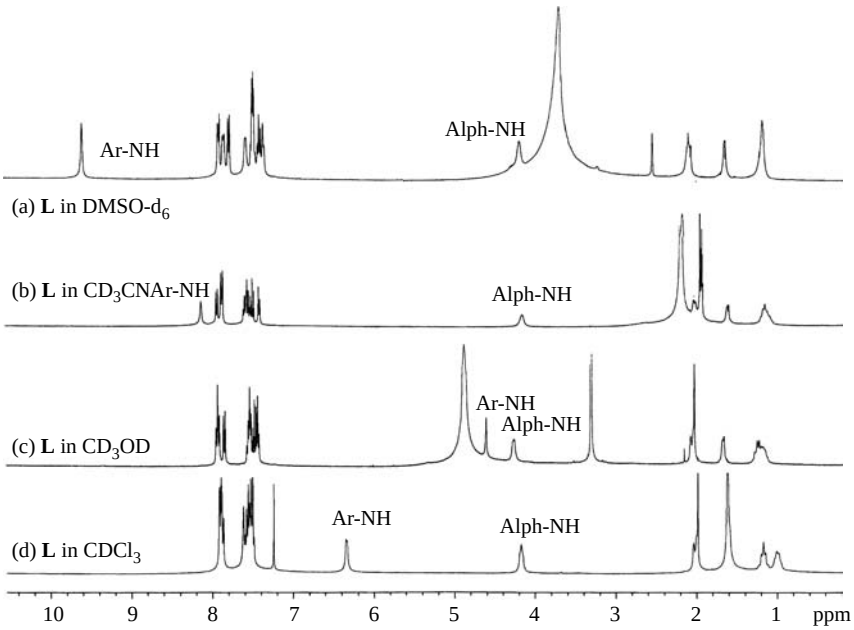

Figure 6. Comparative ^{1}H NMR spectra of (a) DMSO-d_6-solvated *bis*-thiourea; (b) CD_3CN-solvated *bis*-thiourea; (c) CD_3OD-solvated *bis*-thiourea; and (d) $CDCl_3$-solvated *bis*-thiourea system.

of the solvatomorphs. However, the stereochemical assignment of aromatic N—H and aromatic N—H protons of *bis*-thiourea derivative was established on the basis of the NOESY study. The extensive NOESY spectrum showed no significant cross-coupling between aromatic N═H and aromatic N═H protons which suggested the anti arrangement.

Absorption spectroscopy

The UV–vis spectrum of the *bis*-thiourea compound **L** showed two absorption bands (Figure 7). The high intense band at 277 nm in the UV region ($\varepsilon = 8900\,M^{-1}\,cm^{-1}$) may be assigned to the $n \rightarrow \pi*$ transition and a relatively weak intense band at 320 nm ($\varepsilon = 2675\,M^{-1}\,cm^{-1}$) is due to $\pi \rightarrow \pi*$ transition (*22*).

However, it does not show sufficient solvatochromism (see Supplementary Information, available online). On closer inspection, we have noticed that, as the solvent polarity increases (or decreases), a hypsochromic (or bathochromic) shift of λ_{max} ($\sim$5 nm) is observed. A reasonable interpretation is that, upon excitation from the ground state to the electronic excited state, electron density of the negative pole —C═S will be depressed due to the migration of electrons towards the positive pole (carbon atom of the thiourea group). Thus, the dipole moment of the molecule will be decreased after excitation. Therefore, as the solvent polarity increased, the energy depression of the ground state will be more than that of the excited state, and this causes a hypsochromic shift of the spectra (*23*).

Fluorescence spectroscopy

There have been several experimental and theoretical studies on the solvatochromic behaviour of thiourea derivatives (*24*). To investigate the influence of the solvent polarity on the excited state behaviour of the ligand, we have studied the steady state and lifetime emission spectra of **L** in solvents of different polarities. Steady state emission spectrum shows a monomer emission between 387 and 410 nm when excited at 320 nm with varying the solvent polarities (Figure 8(a)). On increasing the solvent polarity from THF to DMF (4.0–6.4), a red shift was observed in maximum emission wavelength. Enhancement

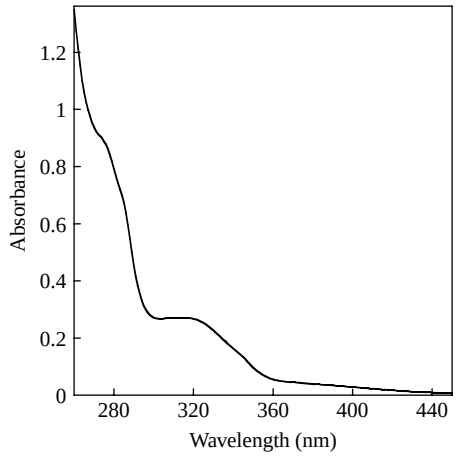

Figure 7. UV–vis spectra of ligand **L** in MeOH solvent.

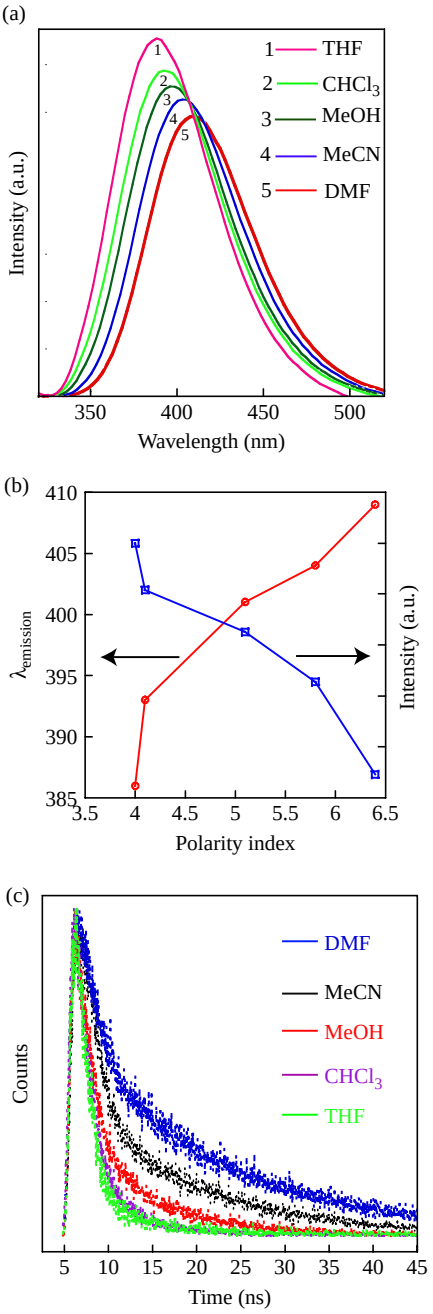

Figure 8. (a) Emission spectra of **L** in different solvents ($\lambda_{ex} = 320$ nm, 1.0×10^{-5} M, 298 K). 1: THF, 2: $CHCl_3$, 3: MeOH, 4: MeCN and 5: DMF; (b) plot of polarity index of different solvents vs. fluorescence intensity and quantum yield of ligand (**L**) and (c) time-resolved fluorescence decay of **L** monitored at the corresponding emission maxima at room temperature in different solvents.

of the solvent polarity causes a significant quenching of the fluorescence spectra (Figure 8(b)). The quantum efficiency (Φ) of the ligand in different solvents follows the order of DMF (0.51) > CH_3CN (0.45) > MeOH (0.42) > $CHCl_3$ (0.37) > THF (0.27) (*25*), which may be attributed to the difference in the non-covalent interactions between solvents and ligand **L** as supported by the crystal structure studies. Time-resolved fluorescence study was performed to investigate the effect of the solvent polarity on emission behaviour of the ligand (Figure 8(c)). In all cases, fluorescence decay was described by a linear combination of two exponential terms and positive pre-exponential factors (Table 2). It has been observed that lifetime (τ_2) value and mean lifetime (τ_m) value change drastically the change in polarity of the solvent. With an increase in the polarity of solvent from THF to DMF, mean lifetime (τ_m) value change over a range 1.106–5.089 ns. It can be concluded that the more polar solvents stabilise the excited state of the host molecule and as a result lifetime increases, which is also supported by the solvent–ligand non-covalent interactions in the solid state.

Conclusions

The flexible *bis*-thiourea compound exhibits pseudo-polymorphism in the solid state due to its inherent tendency to crystallise via forming multiple hydrogen-bonding interactions with various solvent (guests) molecules. The crystal structure and morphology of the ligand is highly influenced by the choice of solvents used in the crystallisation process. Flexible ligand molecule reorganises in the lattice to entrap solvent molecules of different sizes and geometries. The formation of inter-ligand N—H···S type of hydrogen bonds among the host molecules involving *syn* N—H group in all cases is noteworthy. However, due to the restricted disposition of the *anti* N—H group, it can only form weak interactions with the solvent molecules. In DMF-solvated crystal, we have encountered with lp···π interactions, which is a quite uncommon non-covalent interaction hardly reported in the literature. We have studied the solvent-induced polymorphism in these crystals by optical microscopy, powder X-ray diffraction and thermal analysis. From the FT-IR spectra of the compound in the solution phase, the peak corresponding to the respective solvents is broadened compared to that in the solid phase. The ligand was appended with two naphthalene units to ensure the solution phase non-covalent interactions with different solvents using steady and time-resolved fluorescence spectroscopy. In the steady state, increase in the solvent polarity results in a red shift of the emission band from 387 to 410 nm and, consequently, quenching takes place, which possibly results due to increases in the formation of the non-covalent interactions. It has been observed that increasing the solvent polarity increases the lifetime of *bis*-thiourea derivatives (**L**) which is in agreement with the crystal structures displaying non-covalent interaction with solvent molecules. Finally, we can conclude that the fluorescence-quenching phenomenon reveals the presence of various non-covalent interactions between the solvent

Table 2. Fluorescence lifetime parameters of **L** in different solvents.

Solvent	Polarity index	τ_1 (ns)	τ_2 (ns)	α_1	α_2	χ^2	τ_m (ns)
DMF	6.4	0.27	6.70	0.0087	0.026	1.033	5.089
MeCN	5.8	0.36	5.07	0.0036	0.007	1.005	3.470
MeOH	5.1	0.24	2.88	0.0110	0.006	0.999	1.877
$CHCl_3$	4.1	0.11	1.44	0.0101	0.007	0.999	1.190
THF	4.0	0.12	1.73	0.0450	0.071	1.004	1.106

and *bis*-thiourea derivative which were observed in the solid state. From the NMR experiment, we can conclude that a large change (shifted) in peak position of aromatic —NH protons in various solvents is responsible for the pseudo-polymorphic nature of cyclohexane *bis*-thiourea derivative. We are presently extending this result by preparing new thiourea-based fluorescence receptors with novel structural and spectral properties.

Experimental section

Materials and methods

All reagents were obtained from commercial sources and used as received. The IR spectra were recorded on a Perkin–Elmer Spectrum One FT-IR spectrometer with KBr discs in the range of 4000–400 cm^{-1}. The absorption spectra were recorded on a Perkin–Elmer Lambda-25 UV–vis Spectrometer at 298 K. NMR spectra were recorded on a Varian FT-400 MHz instrument. Elemental analyses were carried out on a Perkin–Elmer 2400 automatic carbon, hydrogen and nitrogen analyser. The thermal analyses of the compounds were performed using an SDTA 851 e TGA thermal analyser (Mettler Toledo) with a heating rate of 2°C per min in a N_2 atmosphere. PXRD data were recorded with Seifert powder XRD (3003TT) with Cu K_α source ($\lambda = 1.54$ Å) on a glass surface of an air-dried sample. Optical micrograph images were taken in Zeiss-Axio Cam-MRc microscope fitted with the digital camera. The steady-state fluorescence spectra were recorded on a Varian Cary-Bio spectrofluorimeter and corrected for emission. Fluorescence quantum yield was determined in each case by comparing the corrected spectrum with that of naphthalene ($\Phi_F = 0.23$) (*26*) in ethanol by taking the area under the total emission using the following equation (*27*).

$$\Phi_S = \Phi_R(\Phi_S A_R)/\Phi_R A_S)(\eta_S/\eta_R),$$

where Φ_S and Φ_R are the radiative quantum yields of the sample and the reference, Φ_S and Φ_R are the area under the fluorescence spectra of the sample and the reference, A_S and A_R are the absorbance of the sample and the reference (at the excited wavelength) and η_S and η_R are the refractive indices of the solvent used for the sample and the reference. The quantum yield of naphthalene was measured using quinine sulphate in 1N H_2SO_4 as reference at λ_{ex} of 350 nm ($\Phi_F = 0.54$). Time-resolved intensity decays were measured using a Life Spec II spectrofluorimeter (Edinburgh instrument). The sample was excited by Pico-quant laser source. The decay curves were analysed by the FAST software using the discrete exponential method. The generated curves for intensity decay were fitted in the functions:

$$I_{(t)} = \sum\nolimits_i \alpha_i \exp(-t/\tau_i),$$

where τ_i is the initial intensity of the decay component i, having a lifetime α_i. The mean lifetime (τ_m) of *bis*-thiourea ligand **L** in different experimental conditions was calculated following the equation (*28*):

$$\tau_m = \frac{\sum_i \alpha_i \tau_i}{\sum_i \alpha_i}.$$

X-ray crystallography

The intensity data were collected using a Bruker SMART APEX-II CCD diffractometer, equipped with a fine focus 1.75 kW sealed tube Mo K_α radiation ($\lambda = 0.71073$ Å) at 273(3) K, with increasing ω (width of 0.3°per frame) at a scan speed of 3 s/frame. SMART software was used for data acquisition. Data integration and reduction were undertaken with SAINT and XPREP (*29*) software. Multi-scan empirical absorption corrections were applied to the data using the program SADABS (*30*). Structures were solved by direct methods using SHELXS-97 and refined with full-matrix least squares on F^2 using SHELXL-97 (*31*). All non-hydrogen atoms were refined anisotropically. The hydrogen atoms were located from the difference Fourier maps and refined. Structural illustrations were drawn with ORTEP-3 for Windows (*32*). All the crystallographic data parameters are shown in Table 3.

Synthesis, characterisation of ligand and solvated systems

L was synthesised following the literature procedure (*33*). The crystal quality of the ligand was not so good (Figure S2). The compound was dissolved in the solvent at higher temperature under agitation to get a saturated solution.

Table 3. Crystallographic data for **MeOH-**, **MeCN-** and **DMF**-solvated cyclohexane dinapthyl *bis*-thiourea derivative.

Entry	**L·MeOH**	**L·MeCN**	**L·DMF**
Empirical formula	$C_{29}H_{32}N_4OS_2$	$C_{30}H_{31}N_5S_2$	$C_{31}H_{35}N_5OS_2$
CCDC No.	48434	748435	748436
Fw	516.73	525.74	557.78
Crystal system	Triclinic	Triclinic	Orthorhombic
Space group	*P-1*	*P-1*	*Pna2(1)*
a (Å)	10.9902(7)	10.9411(3)	14.333(2)
b (Å)	11.1720(7)	11.3284(3)	10.7574(18)
c (Å)	12.7825(9)	13.9479(7)	19.502(3)
α (deg)	89.024(4)	111.849(3)	90.00
β (deg)	75.506(4)	94.689(3)	90.00
γ (deg)	65.624(5)	112.682(2)	90.00
V (Å)^3	1377.43(16)	1428.36(9)	3006.9(8)
Z	2	2	4
μ	0.223	0.215	0.208
F(000)	548	532	1184
hkl ranges	$-12 \le h \le 14$	$-13 \le h \le 10$	$-19 \le h \le 19$
	$-13 \le k \le 14$	$-15 \le k \le 14$	$-14 \le k \le 13$
	$-16 \le l \le 16$	$-18 \le l \le 18$	$-25 \le l \le 25$
T_{max}/T_{min}	0.946/0.905	0.946/0.920	0.941/0.915
Data/parameters	6247/0/327	5867/0/336	2412/1/354
GOF(S)	1.023	1.039	0.971
R_{int}	0.0398	0.0418	0.1072
Final *R* indices	$R1 = 0.0531$	$R1 = 0.0489$	$R1 = 0.0424$
$[I > 2\sigma(I)]$	$wR2 = 0.1349$	$wR2 = 0.0557$	$wR2 = 0.0662$
R indices (all data)	$R1 = 0.0852$	$R1 = 0.0864$	$R1 = 0.0577$
	$wR2 = 0.1526$	$wR2 = 0.0623$	$wR2 = 0.0903$

Then, the solvent was allowed to evaporate gradually to get the corresponding solvated crystal at rt. Anal. Calcd (%) for $C_{29}H_{32}N_4OS_2$ (**L·MeOH**): C, 67.41; H, 6.24; N, 10.85 Found: C, 67.44; H, 6.22; N, 10.84%. Anal. Calcd (%) for $C_{30}H_{31}N_5S_2$ (**L·MeCN**): C, 68.54; H, 5.94; N, 13.33 Found: C, 68.56; H, 5.95; N, 13.35%. Anal. Calcd (%) for $C_{31}H_{35}N_5OS_2$ (**L·DMF**): C, 66.75; H, 6.33; N, 12.56 Found: C, 66.78; H, 6.34; N, 12.55%.

NMR data of various solvated dinapthayl bis-thiourea ligand

L. ^{1}H NMR (400 MHz, DMSO-d_6): δ 9.88 (s, 2H, NH), 8.21 (δ, $J = 8.01$ Hz, 2H), 7.93 (δ, $J = 7.5$ Hz, 2H), 7.88 (δ, $J = 7.8$ Hz, 2H), 7.61 (m, 4H), 7.44 (m, 4H), δ 4.22 (s, 2H, NH), 2.2 (m, 2H), 1.66 (m, 2H), 1.27–1.21 (m, 4H); ^{13}C NMR (100 MHz, DMSO-d_6): δ 181.64,134.78, 134.28, 129.95, 128.42, 126.91, 126.49, 126.01, 125.32, 123.42, 123.08, 57.81, 31.95, 24.64.

L·MeOH. ^{1}H NMR (300 MHz, CD_3CN): δ 8.21 (s, 2H, NH), 8.05 (δ, $J = 8.02$ Hz, 2H), 7.96 (δ, $J = 7.4$ Hz, 2H), 7.81 (δ, $J = 7.7$ Hz, 2H), 7.79 (m, 4H), 7.71 (m, 4H), 7.61 ($J = 7.7$ Hz, 2H), δ 4.31 (s, 2H, NH), 2.15 (m, 2H), 1.66 (m, 2H), 1.26–1.11 (m, 4H); ^{13}C NMR (100 MHz, CD_3CN): δ 181.35, 134.98, 134.88, 129.35, 128.62, 126.56, 126.32, 126.11, 125.52, 123.46, 123.19, 57.78, 31.56, 24.68.

L·MeCN. ^{1}H NMR (300 MHz, CD_3OD): δ 4.72 (s, 2H, NH), 8.03. (δ, $J = 8.04$ Hz, 2H), 7.96 (d, $J = 7.4$ Hz, 2H), 7.71 (δ, $J = 7.9$ Hz, 2H), 7.79 (m, 4H), 7.68 (m, 4H), 7.62 ($J = 7.5$ Hz, 2H), δ 4.24 (s, 2H, NH), 2.18 (m, 2H),1.65 (m, 2H), 1.29–1.21 (m, 4H); ^{13}C NMR (100 MHz, CD_3OD): δ 181.53,134.80, 134.47, 129.89, 128.46, 126.88, 126.61, 126.34, 125.29, 123.38, 123.12, 57.86, 31.62, 24.67.

L·DMF. ^{1}H NMR (400 MHz, $CDCl_3$): δ 6.35 (s, 2H, NH), 7.93 (δ, $J = 8.6$ Hz, 2H), 7.91 (δ, $J = 7.5$ Hz, 2H), 7.73 (δ, $J = 7.7$ Hz, 2H), 7.69 (m, 4H), 7.61 ((m, 4H), δ 6.35 (s, 2H, NH), 2.11 (m, 2H), 1.61 (m, 2H), 1.22(m, 2H), 1.01 (m, 2H); ^{13}C NMR (100 MHz, 400 MHz, $CDCl_3$): δ 181.22, 134.65, 134.32, 129.93, 128.47, 126.85, 126.43, 126.07, 125.21, 123.57, 123.05, 57.51, 31.84, 24.61.

Acknowledgements

GD acknowledges DST (SR/S1/IC-01/2008) and CSIR (01-2235/08/EMR-II), New Delhi, India, for financial support and DST-FIST for single-crystal X-ray diffraction facility. AP wishes to thank CSIR for JRF (09/731(0045)/2007-EMR –I).

References

(1) (a) Bernstein, J. *Polymorphism in Molecular Crystals*; Oxford University Press: New York, 2002. (b) Brittain, H.G. *Polymorphism in Pharmaceutical Solids*; Marcel Dekker: New York, 1999.

(2) (a) Kobayashi, K.; Sato, K.; Sakamoto, S.; Yamaguchi, K. *J. Am. Chem. Soc.* **2003**, *125*, 3035–3045. (b) Jetti, R.K.R.; Boese, R.; Thallapally, P.K.; Desiraju, G.R. *Cryst. Growth Des.* **2003**, *6*, 1033–1042. (c) Plass, K.E.; Kim, K.; Matzger, A. *J. Am. Chem. Soc.* **2004**, *126*, 9042–9053. (d) Ahn, S.; Kariuki, B.M.; Harris, K.D.M. *Cryst. Growth Des.* **2001**, *1*, 107–111.

(3) (a) Atwood, J.L.; Davies, J.E.D.; MacNicol, D.D. *Inclusion Compounds*; Oxford University Press: Oxford, 1991. (b) Hollingsworth, M.D. *Science*, **2002**, *295*, 2410–2413. (c) Desiraju, G.R. *Crystal Engineering the Design of Organic Solids*, Elesevier: Amsterdam, 1989.

(4) Desiraju, G.R. *Crystal Engineering The Design of Organic Solids*; Elesevier: Amsterdam, 1989.

(5) (a) Weissbuch, I.; Torbeev, V.Y.; Leiserowitz, L.; Lahav, M. *Angew. Chem. Int. Ed.* **2005**, *117*, 3290–3293. (b) Lee, A.Y.; Lee, I.S.; Mersmann, A.; *Chem. Eng. Technol.* **2006**, *29*, 281–285. (c) Heinrich, J.; Ulrich, J. *The 16th International Symposium on Industrial Crystallization*; A-13 Dresden, Germany, 2005; Vol. 9, 11–14.

(6) (a) Horner, M.J.; Holman, K.T.; Ward, M.D. *Angew. Chem., Int. Ed.* **2001**, *40*, 4045–4048. (b) MacGillivray, L.R.; Reid, J.L.; Ripmeester, J.A. *Chem. Commun.* **2001**, 1034–1035. (c) Kobayasi, K.; Sato, A.; Sakamoto, S.; Yamaguchi, K. *J. Am. Chem. Soc.* **2003**, *125*, 3035–3045.

(7) (a) Akutagawa, T.; Koshinaka, H.; Ye, Q.; Noro, S.-I.; Kawamata, J.; Yamaki, H.; Nakamura, T. *Chem. Asian J.* **2010**, *5*, 520–529. (b) Nangia, A.; Desiraju, G.R.; *Chem. Commun.* **1999**, 605–606.

(8) (a) Amendola, V.; Boiocchi, M.; Fabbrizzi, L.; Mosca, L. *Chem. Eur. J.* **2008**, *14*, 9683–9696. (b) Jordan, B.J.; Pollier, M.A.; Miller, L.A.; Tiernan, C.; Clavier, G.; Audebert, P.; Rotello, V.M.; *Org. Lett.* **2007**, *9*, 2835–2838. (c) Han, J.; Zhao, L.; Yau, C.-W.; Mak, T.C.W. *Cryst. Growth Des.* **2009**, *1*, 308–319.

(9) (a) Wishkerman, S.; Bernstein, J.; Hickey, M.B. *Cryst. Growth Des.* **2009**, *9*, 3204–3210. (b) Zuend, S.J.; Jacobsen, E.N. *J. Am. Chem. Soc.* **2009**, *31*, 15358–15374. (c) Guez-Lucena, D.R.; Mellet, C.O.; Jaime, C.; Burusco, K.K.; Fernndez, J.M.G.; Benito, J.M. *J. Org. Chem.* **2009**, *74*, 2997–3008.

(10) (a) Nagy, E.; Mihalik, R.; Hrabak, A.; Vertesi, C.; Gergely, P. *Immunopharmacology* **2000**, *47*, 25–33. (b) Shamim, A.; Satoshi, K.; Kiyohisa, O.; Takayuki, M.; Yoko, T. *Talanta* **1999**, *48*, 63–69.

(11) (a) Liu, W.-X.; Jiang, Y.-B. *J. Org. Chem.* **2008**, *73*, 1124–1127. (b) Woller, E,K.; Walter, E.D.; Morgan, J.R.; Singel, D.J.; Cloninger, M.J. *J. Am. Chem. Soc.* **2003**, *125*, 8820–8826.

(12) (a) Zuend, S.J.; Jacobsen, E.N. *J. Am. Chem.* **2009**, *131*, 15358–15374. (b) Pfeffer, F.M.; Gunnlaugsson, T.; Jensen, P.; Kruger, P.E. *Org. Lett.* **2005**, *7*, 5357–5360.

(13) (a) Jetti, R.K.R.; Boese, R.; Thallapally, P.K.; Desiraju, G.R. *Cryst. Growth Des.* **2003**, *3*, 1033–1040. (b) Nangia, A. *Cryst. Growth Des.* **2006**, *6*, 1278–1281. (c) Zhang, Z.; Knobler, C.B. Hawthorne, M.F. *J. Am. Chem. Soc.* **1995**, *117*, 5105–5113. (d) Choi, K.; Hamilton, A.D. *Coord. Chem. Rev.* **2003**, *240*, 101–110. (e) Bondy, C.R.; Loeb, S.J. *Coord. Chem. Rev.* **2003**, *240*, 77–99.

(14) (a) Pramanik, A.; Das, G. *Tetrahedron* **2009**, *65*, 2196. (b) Pramanik, A.; Bhuyan, M.; Das, G. *J. Photochem. Photobiol. A Chem.* **2008**, *197*, 149–155. (c) Pramanik, A.; Bhuyan, M.; Choudhury, R.; Das, G. *J. Mol. Struct.* **2008**, *879*, 88–95. (d) Das, G.; Bharadwaj, P.K.; Basu Roy, M.; Ghosh, S. *Chem. Phys.* **2002**, *277*, 145–160.

(15) Wang, W.-H.; Xi, P.-H.; Su, X.-Y.; Lan, J.-B.; Mao, Z.-H.; You, J.-S.; Xie, R.-G. *Cryst. Growth Des.* **2007**, *7*, 741–746.

(16) Tobe, Y.; Sasaki, S.; Mizuno, M.; Hirose, K.; Naemura, K. *J. Org. Chem.* **1998**, *63*, 7481–7489.

(17) Muthu, S.; Vittal, J.J. *Cryst. Growth Des.* **2004**, *4*, 1181–1184.

(18) Egli, M.; Sarkhel, S. *Acc. Chem. Res.* **2007**, *40*, 197–205.

(19) Mooibroek, T.J.; Gamez, P.; Reedijk, J. *Cryst. Eng. Commun.* **2008**, *10*, 1501–1510.

(20) Srinivasan, K.; Sankaranarayanan, K.; Thangavelu, S. *J. Cryst. Growth* **2000**, *212*, 246–254.

(21) (a) Qing, G.-Y.; Sun, T.-L.; Wang, F.; He, Y.-B.; Yang, X. *Eur. J. Org. Chem.* **2009**, 841–849. (b) Sansone, F.; Chierici, E.; Casnati, A.; Ungaro, R. *Org. Biomol. Chem.* **2003**, *1*, 1802–1809.

(22) Kondo, S.-I.; Sato, M. *Tetrahedron* **2006**, *62*, 4846–4850.

(23) (a) Zhou, J.W.; Li, Y.T.; Tang, Y.W.; Song, X.Q. *J. Solution Chem.* **1995**, *24*, 925–933. (b) Reichardt, C. *Solvents and Solvent Effect in Organic Chemistry*, 2nd ed., VCH: Weinheim, 1988.

(24) (a) Brooker, L.G.S.; Keys, C.H.; Heseltine, D.W. *J. Am. Chem. Soc.* **1951**, *73*, 5350–5356. (b) Reichardt, C. *Solvents and Solvent Effects in Organic Chemistry*; Chemie: New York 1988. (c) Reichardt, C. *Chem. Rev.* **1994**, *94*, 2319–2358.

(25) (a) Nekipelova, T.D.; Shishkov, V.S. *High Energy Chem.* **2004**, *38*, 353–355. (b) Changa, C.-C.; Chua, J.-F.; Kuoa, H.-H.; Kanga, C.-C.; Lina, S.-H.; Changa, T.-C. *J. Lumin.* **2006**, *119–120*, 84.

(26) Birks, J.B. *Photophysics of Aromatic Molecules*; Wiley-Interscience: New York, 1970.

(27) Uchiyama, S.; Matsumura, Y.; de Silva, A.P.; Iwai, K. *Anal. Chem.* **2003**, *75*, 5926–5935.

(28) Swaminathan, R.; Krishnamoorthy, G.; Periasamy, N. *Biophys. J.* **1994**, *67*, 2013–2023.

(29) *SMART, SAINT and XPREP*; Siemens Analytical X-ray Instruments, Inc.: Madison, WI, 1995.

(30) Sheldrick, G.M.;, SADABS: *Software for Empirical Absorption Correction*, University of Gottingen, Institute fur Anorganische Chemieder Universitat, Tammanstrasse 4, D-3400 Gottingen, Germany, 1999–2003.

(31) Sheldrick, G.M. *SHELXS-97*; University of Gottingen: Germany, 1997.

(32) Farrugia *J. Appl. Crystallogr.* **1997**, *30*, 565–566.

(33) (a) Xie, H.; Yi, S.; Wu, S. *J. Chem. Soc. Perkin Trans.* **1999**, *2*, 2751–2162. (b) Costero, A.M.; Colera, M.; Gavina, P.; Gil, S.; Llaosa, U. *Tetrahedron* **2008**, *64*, 7252–7257.